

Plutonium-238 Production Sensitivity and Validation Studies Continued: Effects of Core Component Compositions¹

D. Chandler,* D. Hartanto, J. W. Bae, K. M. Burg, and Y. E. Robert

*Oak Ridge National Laboratory, P.O. Box 2008, Oak Ridge, TN 37831-6170, USA, *chandlerd@ornl.gov*

INTRODUCTION

This paper presents the results from a series of ^{238}Pu production sensitivity and validation studies, expanding on the research documented in previous work by Chandler et al. [1]. In support of the ^{238}Pu Supply Project (PSP), the High Flux Isotope Reactor (HFIR) irradiates NpO_2/Al pellets to produce ^{238}Pu , which is used as a power source for National Aeronautics and Space Administration (NASA) missions. The aforementioned study evaluated the effects of temporal meshes, target spatial meshes, and target temperatures on ^{238}Pu production metrics based on Campaign 6 irradiation and measurement data. The primary purpose of this second study is to evaluate the effects of Be reflector and control element (CE) compositions on k_{eff} and ^{238}Pu production metrics. Shift [2,3] is used for neutron transport and depletion calculations and ORIGEN [2] is used for isotopic evolution calculations outside of Shift.

Reactor Design and Missions

HFIR is a US high-performance research reactor (USHPRR) operated at Oak Ridge National Laboratory (ORNL) on behalf of the US Department of Energy (DOE). World-leading facilities such as HFIR and the Radiochemical Engineering Development Center make ORNL an ideal lab for the production of ^{238}Pu . HFIR's mission portfolio of neutron scattering, isotope production, materials irradiation, fuels irradiation, neutron activation analysis, and other radiation-based research is attributed to its core design (Fig. 1) and high power density.

HFIR is a pressurized, light-water reactor that operates at 85 MW_{th} for ~24–26 day cycles. Its fuel assembly (FA) consists of two concentric fuel elements, each holding hundreds of involute-shaped fuel plates containing highly enriched uranium ($\text{U}_3\text{O}_8\text{-Al}$, ~93 wt %). A central flux trap nested inside the FA and a large ring of Be on the outside of the FA house in-core experiment facilities. Two concentric CEs—each containing gray (Ta-Al) and black ($\text{Eu}_2\text{O}_3\text{-Al}$) longitudinal regions—are located between the FA and Be reflector and are withdrawn axially during the cycle. The reflector is subdivided into the removable Be (RB), the semi-permanent Be (SPB), control rod access plugs (CRAPs), and the permanent Be (PB) reflectors.

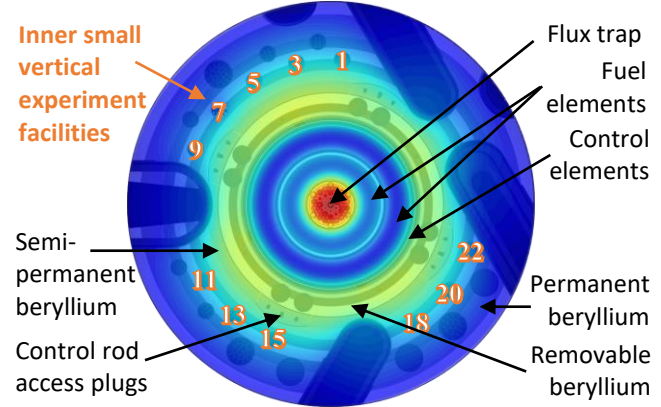


Fig. 1. HFIR core model and thermal flux distribution [1].

Descriptions of Projects

The purpose of the PSP is to establish and maintain a domestic supply of ^{238}Pu to power NASA deep-space and planetary missions. NASA uses radioisotope power systems to convert the decay heat emanating from PuO_2 pellets into electrical power. Targets containing NpO_2/Al pellets are irradiated in PB vertical experiment facilities (VXFs) to produce ^{238}Pu . Thus, ^{238}Pu sensitivity and validation studies are important to PSP for efforts such as enhancing production yield estimates and continued target design optimization.

Staff at ORNL also collaborate with DOE's National Nuclear Security Administration (NNSA) Office of Material Management and Minimization (M3) in support of their nonproliferation goal to convert the remaining USHPRRs to LEU fuel. Moreover, maintaining or enhancing HFIR's capabilities is an important conversion objective. This study is therefore important for LEU conversion in determining baseline metrics with the HEU core to use in near-future HEU-to-LEU comparison studies.

Summary of First Study Findings

A systematic progression of sensitivity studies assessing the effects of the modeled temporal mesh, target spatial mesh, and target temperature on ^{238}Pu production was performed in [1]. The Shift tool was used with a modified version of the representative model [4] and ENDF/B-VII.1 cross sections [5]. Five cases simulating 10, 13, 16, 19, and 25 depletion

¹ Notice: This manuscript has been authored by UT-Battelle, LLC, under contract DE-AC05-00OR22725 with the US Department of Energy (DOE). The US government retains and the publisher, by accepting the article for publication, acknowledges that the US government retains a nonexclusive, paid-up, irrevocable, worldwide license to publish or reproduce the published form of this manuscript, or allow others to do so, for US government purposes. DOE will provide public access to these results of federally sponsored research in accordance with the DOE Public Access Plan (<http://energy.gov/downloads/doe-public-access-plan>).

steps throughout each of the ~25-day irradiation cycles were executed, and trivial differences were observed between the production results. Then, 27 unique spatial meshes (1–198 NpO₂/Al spatial cells per axial stack of pellets) were modeled, and all the ²³⁸Pu mass results were within 1%. Lastly, temperatures of 293.6 K and 400–1,200 K, in 100 K increments, were evaluated, and trivial differences were again observed. The production studies in [1] overpredicted the Campaign 6 mass measurement by approximately 2–9% depending on the modeling and mass recovery assumptions.

STUDY METHODS AND DATA

The Shift code was used for continuous-energy Monte Carlo–based neutron transport and depletion simulations using SCALE Version 7.0 Beta 7. The reference neutronics inputs include the simplified fuel and representative experiment loading model [4] and the ²³⁸Pu production validation models documented in [1]. All transport calculations used ENDF/B-VII.1 cross section libraries. Standalone SCALE 6.3.1 ORIGEN calculations were performed to generate cross section libraries and to activate reactor component materials of interest.

Campaign 6 Data

The Campaign 6 data discussed in [1] are summarized here for completeness. Full-length targets consisting of 52 NpO₂/Al pellets were irradiated in VXF 1, 3, 5, 11, 13, 15, 18, 20, and 22 during cycles 486 (25.01 days) and 487 (25.14 days). Each VXF holder consists of 7 targets, and thus 63 targets were irradiated. Pellets are nominally composed of 20 vol % NpO₂ and 70 vol % Al, with the remainder being void. As-fabricated pellet data (e.g., dimensions and compositions) were used in these studies. A mass of 166.39 g²³⁸Pu (2.64 g/target) was recovered, and a maximum mass of ~175.15 g (2.78 g/target) is assumed based on a conservatively low assumed recovery fraction of 0.95.

TRANSMUTATION PATHS

The production of ²³⁸Pu in the irradiation targets, ³He and ⁶Li in the Be reflector, and ¹⁸²Ta in the CEs are important in this study, as are composition evolutions in the fuel plates. Plutonium-238 is produced via neutron capture in ²³⁷Np and subsequent beta decay of ²³⁸Np (Fig. 2).

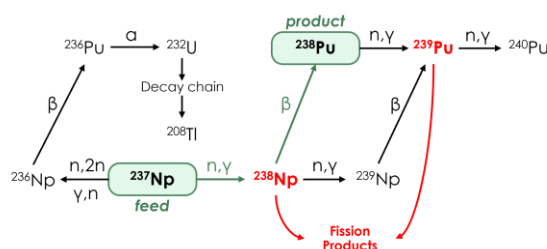


Fig. 2. Plutonium-238 production path.

Irradiation of the CEs' gray regions transmutes ¹⁸¹Ta to ¹⁸²Ta ($t_{1/2}=114.74$ days), which has a much greater absorption cross section. Irradiation of the Be reflector results in small quantities of ³He and ⁶Li (Fig. 3), which have very large thermal absorption cross sections.

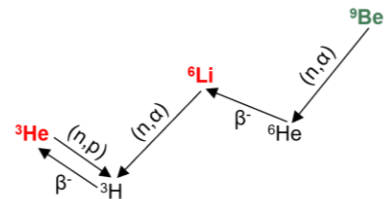


Fig. 3. Helium-3 and ⁶Li production path.

Control Element and Beryllium Activation

In the first study models, the CE gray and black regions were modeled as fresh, unirradiated materials at the beginning of the analyzed cycles. The RB was modeled as fresh, unirradiated materials, whereas the SPB, CRAP, and PB contained small amounts of ³He and ⁶Li based on representative irradiated conditions and methods developed in Ilas [6]. The CE materials were activated during the Shift simulations, but the reflector was not. The k_{eff} values near beginning-of-cycle (BOC) were high (~1.02), and the ²³⁸Pu production results were greater than the measurement. Thus, increased absorption effects caused by ³He, ⁶Li, and ¹⁸²Ta on k_{eff} and ²³⁸Pu production are investigated in this study. A new method, described in Fig. 4, was developed to generate time-dependent CE and Be compositions.

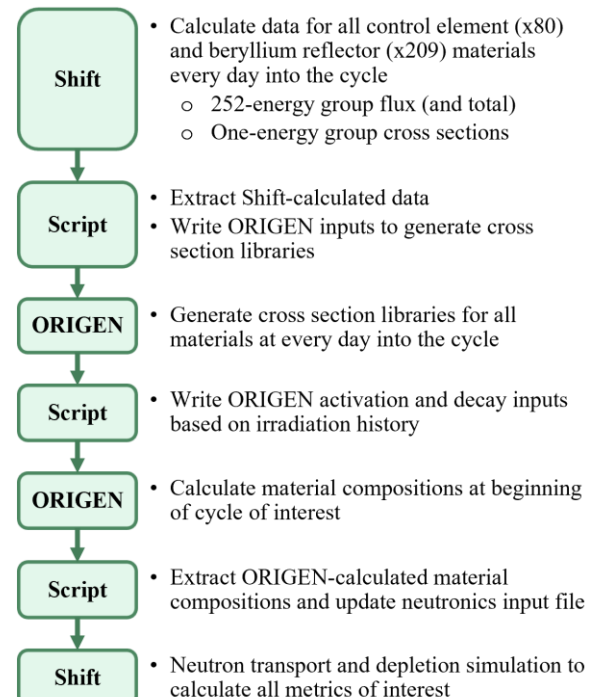


Fig. 4. CE and Be activation method flowchart.

Although Shift is computationally efficient, it is not practical to run tens to possibly hundreds of high-fidelity cycle simulations to estimate CE and Be compositions. Thus, to mitigate the computational time requirements, the method described in Fig. 4 was implemented. First, the reflector geometry was radially and axially segmented to capture the 2D poison concentration distribution. The reflector consists of 3 RB radial cells, 1 SPB radial cell, 1 CRAP radial cell, and 7 PB radial cells. Then, they were axially discretized into 13 zones. Beryllium plugs in the RB and PB were also axially discretized. Ultimately, a total of 209 depletable beryllium cells were modeled in the reflector. The CE gray and black regions were already discretized into 40 unique cells each.

The Shift representative model was executed for a single cycle to calculate the time- and space-dependent neutron fluxes and cross sections. ORIGEN activation/decay libraries were then generated for each cell at each day into the cycle based on the Shift-calculated data. Then, ORIGEN was executed with the applicable irradiation histories to obtain the approximate compositions at the beginning of the cycle of interest, and these compositions were inserted into Shift to perform the subsequent transport and depletion simulations.

STUDY RESULTS

Four Shift multicycle simulations were performed, and their results were compared to the reference case (*Ref.*) results from Chandler et al. [1]. The three new validation cases, referred to as *Val.1*, *Val.2*, and *Val.3*, modeled CE and Be compositions as calculated by the Fig. 4 workflow based on their actual irradiation histories. For comparison purposes, another case, referred to as *Clean*, was executed with fresh, unirradiated CE and Be materials.

The CE materials were activated in all Shift simulations. The Be materials were activated in *Val.1*; however, the isotopic trends (i.e., ^6Li mass vs. time) were not as expected; ^9Be was ignored in the Shift depletion simulation because of the use of $\text{Be S}(\alpha, \beta)$ (i.e., bound Be). Shift activated all the Be material isotopic impurities but did not add ^9Be to the list of isotopes to activate because of the logic in Shift. This issue has been reported to the Shift development team and is being investigated. Therefore, the *Val.2* case did not use $\text{Be S}(\alpha, \beta)$ and activated the Be materials. The *Val.3* case did use $\text{Be S}(\alpha, \beta)$ but did not activate the Be materials.

Composition Variation with Irradiation Time

The variations of ^3He and ^6Li in the Be regions during the two Shift cycles (i.e., cycles 486 and 487) are illustrated in Fig. 5. The ^3He concentrations were greatest for the *Val.3* case because its removal mechanism (Fig. 3) was not simulated. The ^6Li concentrations were greatest for the *Val.2* case because its generation during the cycle was simulated.

Fig. 6 illustrates the ^{181}Ta and ^{182}Ta curves as the sum of all the CE gray materials. The three *Val.* cases were observed to have much less ^{181}Ta than the other cases because the CEs

were irradiated for many cycles. Tantalum-182 at BOC was present in the three *Val.* cases, unlike the other two cases; however, more ^{182}Ta was present in the *Ref.* and *Clean* cases after ~ 5 days into irradiation.

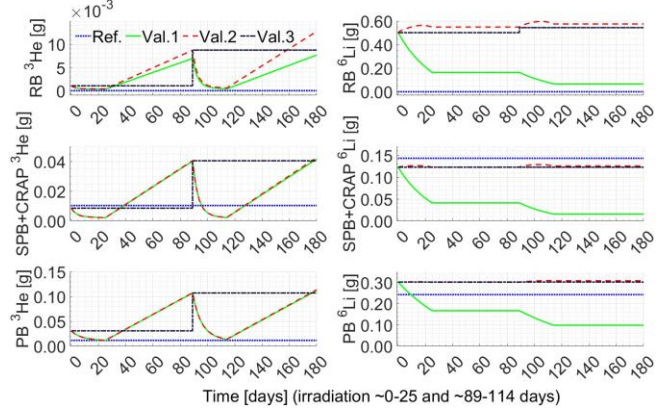


Fig. 5. Helium-3 and ^6Li mass variation with time curves.

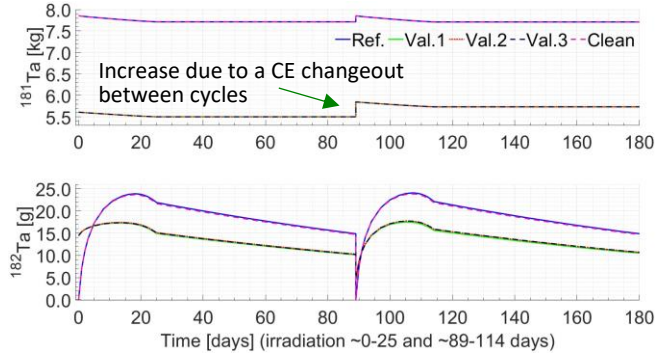


Fig. 6. Tantalum-181 and ^{182}Ta mass variation with time curves.

Effect of Compositions on Reactivity

The time-dependent k_{eff} curves are illustrated in Fig. 7. The as-run CE positions from cycles 486 and 487 were simulated in these studies, and the BOC k_{eff} value for the *Ref.* case was higher than desired ($\sim 2,000$ pcm excess reactivity). Better poison estimates resulted in values closer to unity.

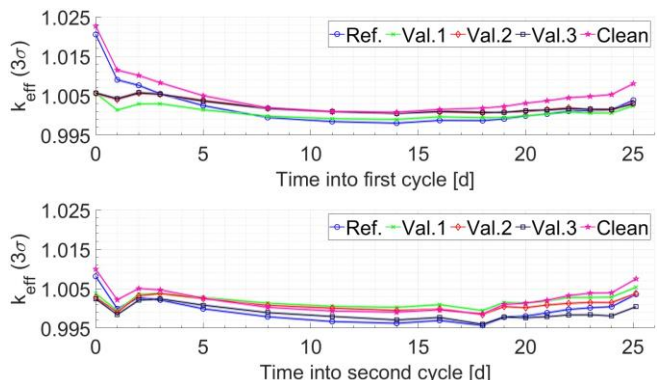


Fig. 7. Variation of k_{eff} with time into cycle.

Effect of Compositions on ^{238}Pu Metrics

Plutonium-238 production masses and qualities (i.e., ^{238}Pu -to-Pu ratio) are shown in Fig. 8. The *Ref.* case produced a mass of 2.87 g/target, and the *Clean* case yielded a 4% greater mass (2.99 g/target). The *Val.3* case produced a mass of 2.80 g/target, which is ~6% greater than the measured result but within 1% if a 0.95 recovery fraction is assumed. The calculated masses ranged from 2.80 to 2.99 g/target. Thus, the Be composition and activation assumptions have greater nontrivial effects on ^{238}Pu production metrics than do the parameters evaluated in the first study (i.e., temporal mesh, spatial mesh, target temperature).

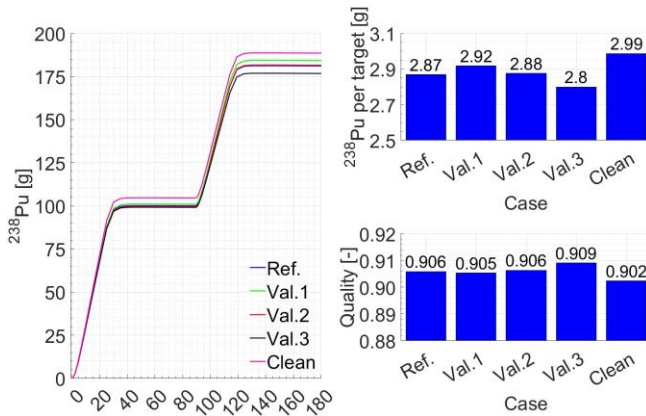


Fig. 8. Plutonium-238 production masses and quality comparisons.

Furthermore, the VXF-dependent average discharge cumulative fission densities are compared to the *Ref.* case in Fig. 9. Fission rate densities and cumulative fission densities are important metrics to characterize in-core behavior and post-irradiation examination results. The increased neutron fluxes incurred in the *Clean* case resulted in fission densities ~10–11% greater than those of the *Ref.* case, whereas the flux reductions incurred in the *Val.3* case resulted in fission densities ~6–7% lower than the *Ref.* case.

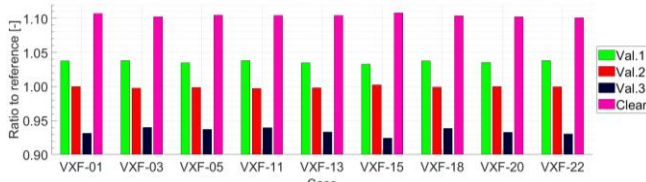


Fig. 9. Fission density ratios relative to reference case.

CONCLUSIONS AND FUTURE WORK

A new computational method was developed to better model CE and Be compositions for the purpose of ^{238}Pu production calculations. The ORNL Shift and ORIGEN codes were used primarily for neutron transport simulations,

cross section library generation, and isotopic evolution calculations. This paper presents a continuation of the studies documented in Chandler et al. [1], which evaluated ^{238}Pu metric sensitivities to temporal meshes, target spatial meshes, and target temperatures. The results presented in this paper indicate that CE and Be compositions—which affect flux to the targets—have a greater effect than the previous study’s parameters. Depending on the composition assumptions, 2.80–2.99 g ^{238}Pu /target was calculated, which is 6–13% greater than the measurement (~1–8% assuming a 0.95 recovery fraction).

Future efforts may focus on other irradiation campaigns, data libraries, and depletion tools (e.g., HFIRCON). Then, a detailed 85 MW HEU to 95 MW LEU core comparison will be performed to characterize the effects of conversion on HFIR’s important ^{238}Pu production mission.

ACKNOWLEDGMENTS

This research was performed on HFIR, a DOE-SC User Facility operated by ORNL under contract DE-AC05-00OR22725. This research was supported by DOE NNSA’s Office of M3, NASA’s Science Mission Directorate, and DOE’s Office of Nuclear Infrastructure Programs. The authors acknowledge C. Sizemore, ORNL LEU conversion manager, and A. Parkison, ORNL PSP manager, for their support. The author’s thank T. Greene, J. Batson, H. Green, and E. Asano for their reviews of this paper.

REFERENCES

1. D. CHANDLER, D. HARTANTO, J. BAE, K. BURG, and Y. ROBERT, “Sensitivity and Validation Studies of Plutonium-238 Production with Shift and ORIGEN,” *Trans. ANS Annual 2024* (2024).
2. W. WIESELQUIST and R. LEFEBVRE, Eds., *SCALE 6.3.1 User Manual*, ORNL/TM-SCALE-6.3.1 (2023).
3. T. PANDYA, S. JOHNSON, T. EVANS, et al., “Implementation, Capabilities, and Benchmarking of Shift, a Massively Parallel Monte Carlo Radiation Transport Code.” *J. Comp. Phys.* **308**, 239–272 (2016).
4. D. CHANDLER, B. BETZLER, E. DAVIDSON, and G. ILAS, “Modeling and Simulation of a High Flux Isotope Reactor Representative Core Model for Updated Performance and Safety Basis Assessments,” *Nucl. Eng. Des.*, **366**, 110752 (2020).
5. M.B. CHADWICK, et al., “ENDF/B-VII.1 Nuclear Data for Science and Technology: Cross Sections, Covariances, Fission Product Yields and Decay Data,” *Nuclear Data Sheets*, **112**, 2887–2996 (2011).
6. D. ILAS, *Impact of HFIR LEU Conversion on Beryllium Reflector Degradation Factors*, ORNL/TM-2013/441 (2013).